P8.20 TYPHOON RAIN RETRIEVALS USING TMI, AMSU-A, AND ISLAND GAUGE DATA SETS

Ching-Chung Li, Wann-Jin Chen, Yung-Chang Chen, Jen-Chi Hu, and Ming-Da Tsai
Chung Cheng Institute of Technology, National Defense University, Taoyuan, 335, Taiwan

1. INTRODUCTION

Numerous disasters, such as flash floods and mudslides, occur in Taiwan owing to Typhoon induced heavy rainfall. Unfortunately, information on rainfall caused by Typhoon is scarce due to a lack of sea-based meteorological radar and rain gauges. Therefore, other methods for accurately estimating the rainfall rate over sea areas are urgently required to reduce losses from heavy rainfall associated with Typhoon. Satellite rainfall retrieval can provide rainfall estimates more frequently and over a wider area than conventional rain gauge measurements, and so can assist in detecting heavy rain events caused by Typhoon. Passive microwave (MW) radiometers can physically sense drops and hydrometeors within precipitating clouds. Therefore, MW rain estimates are widely used in both flash flood monitoring and oceanic heavy rainfall warnings. As a polar molecule, water has a very large dielectric constant at microwave frequencies. This property accounts for the high reflectivity (low emissivity) of the ocean surface (Wilheit and Chang, 1980). The low emissivity of the ocean surface provides a good cold background for viewing particles with relatively higher emissivities, such as rain, over the ocean. Consequently, emission rainfall algorithms rely upon the amount of extra radiation emitted by the precipitation particles against a radiometrically cold background (namely: the ocean) for retrieving rain rates (RRs). In contrast, land surfaces have emissivities in the range of 0.8~0.95 range, and thus emission rainfall algorithms are unsuitable for overland applications, because the high surface emissions effectively mask the precipitation attenuation. On the other hand, scattering rainfall algorithms rely on the general cooling in the high-frequency channels due to the scattering by ice in the upper portions of many raining clouds. Establishing the relationship between the increased MW Tbs and hourly RRs for emission rainfall algorithms, or between decreased Tbs and RRs for scattering rainfall algorithms, require utilizing a theoretically derived relationship between Tbs and RRs or applying regression techniques to ground-truth data.

*_Corresponding author address_: Li, Ching-Chung, Dept. of Computer Science, 190, Shanyuan 1st St., Tahsi, Taoyuan, 335, Taiwan; e-mail: ocean@ccit.edu.tw

Island rain gauge data can be used as ground-truth data coincident with satellite rainfall observations (Chen and Li, 2000). Rainfall observations were treated as representing the rainfall for the waters around the island (or island gauge). MW data from the AMSU-A onboard the NOAA satellites were used in this study to estimate oceanic RRs.

In this study, TRMM Microwave Imager (TMI) level-1B01 data, AMSU-A microwave data, and island gauge measurements from seven isolated islands near Taiwan were used to retrieve Typhoon rainfalls over oceans near Taiwan. One of the main purposes of this study is to establish statistical relationships between them. Several methods of correlating satellite microwave measurements to the observed island gauge data were tried, and a method involved the use of multiple linear regression to compute determination coefficients using the island gauge data as well as passive microwave multiple-channel data from either TMI or AMSU-A was adopted in this paper. This method allowed for the inclusion of different rainfall mechanisms (scattering-based and emission-based rainfall mechanisms), which had been found to be important factors in rain retrievals using passive microwave measurements. The island gauge data were treated as ground truth. The validation results show AMSU rain retrievals overestimate TMI rain retrievals. The multi-sensor technique established in this study was suitable to study the characteristics of typhoon rainfalls, especially for the analyses of rain intensities and rain distributions under cloud tops over oceans. The study results also are helpful for understanding the physical processes within typhoon rain bands, especially for those studies about data assimilation and model simulation. Ground based radar observations are expected in further research, which contribute to establish a typhoon rainfall observation net-work monitoring typhoons continuously.

2. DATASETS AND ALGORITHM

2.1 *Datasets*

This study used four data sets: (1) AMSU-A passive microwave measurements/NOAA-15, -16, (2) IR measurements from the AVHRR (Advanced Very High Resolution Radiometer)/NOAA-15, -16, (3) MV measurements from the TMI, and (4) rainfall

accumulation (mm) over one hour from island rain gauges. These data were obtained from nine different islands in Japan, and were provided by the Japan Meteorological Agency (JMA). Moreover, the AMSU-A and AVHRR satellite data come from NOAA/NESDIS (National Oceanic and Atmospheric Administration/ National Environmental Satellite, Data, Information Service).

The AMSU-A is a 15-channel temperature sounder that operates at frequencies from 23.8 to 89.0 GHz. All AMSU-A channels have a fine resolution of 48 km (compared to 110 km for the MSU) at their nadir with window channels at 23.8, 31.4, 50.3 and 89.0 GHz, representing the primary channels used to retrieve oceanic RR. The AMSU-A has an instantaneous field of view (FOV) of 3.3^{o} at the half-power point, providing a cross-track, scanning $+48.33^{o}$ (-48.33^{o}) from the nadir with a total of 30 FOV (as opposed to 11 for the MSU) per scan line, and completes one scan every eight seconds.

The rain flag (RF) rain identification technique presented by Grody *et al*. (1999) was employed to screen raining regions over the ocean. A parameter called Cloud Liquid Water (CLW) was defined for weather classification, and is shown as below:

$$CLW = CosZ * (A + B * Log(285 - Tb23) + C * Log(285 - Tb31))$$

$$A = 8.24 - (2.622 - 1.846 * Cos\,Z) * Cos\,Z$$

$$B = 0.754$$

$$C = -2.265$$

where Z denoted the zenith angle. According to the thresholds for CLW, all AMSU-A measurements were separated into one of the two rain flag (RF) categories: raining ($CLW > 0.3$) and nonraining ($CLW \leq 0.3$), represented by RF values of 1 and 0 respectively. According to the scattering characteristics of Channel 15 of the AMSU-A at 89.0 GHz, Grody *et al*. also introduced another parameter: Scattering Index over Water (SIW) in order to screen oceanic raining regions. This parameter is shown as below:

$$SIW = -113.2 + (2.41 - 0.0049 * Tb23) * Tb23 + 0.454 * Tb31 - Tb89$$

According to the thresholds for SIW, all AMSU-A measurements were separated into one of the two rain flag (RF) categories: raining ($SIW > 9$) and nonraining ($SIW \leq 9$), which were represented by RF values of 1 and 0 respectively.

AVHRR data were used to avoid the beam-filling problem by discarding inhomogeneous precipitating AMSU-A pixels. Since the AMSU-A and AVHRR were both on the same satellite, no time difference existed between them. Additionally, the horizontal spatial resolution of AVHRR pixel is much better than that of AMSU-A. Accordingly, sufficient AVHRR pixels exist within the footprint of an AMSU-A pixel to distinguish the homogeneous and inhomogeneous field of view. In this study, the AVHRR pixels were superimposed on the footprint of AMSU-A pixel and a supervised classification method was used (Richards and Jia, 1999) to identify the weather conditions (raining or nonraining), conducted by monitoring the AVHRR IR image pattern (cloud distribution) within an AMSU-A raining pixel. This is a very important procedure for verifying whether the rain gauge was located on the edge of a cumulonimbus cloud. If the rain gauge was so located, the beam-filling problem can be said to have occurred, and the RR retrieval result will be uncorrected.

The TRMM satellite was launched in November of 1997 (Kummerow *et al*., 1998), and its inclination to the Equator is 35-degree. The TMI scans the earth with a conical mode, and its antenna beam observes the earth 49 degrees away from nadir, which an incident angle of about 52.8^{o} at the earth's surface. It rotates about the nadir axis at a constant speed of 31.6 rpm, looking forward. Only 130^{o} of the forward sector of every scan is used for getting data. The other sectors are used for calibration and sweep clean data. It takes about 1.9 second for each scan. The TRMM's lower-altitude orbit (350 km and 402 km before and after August 2001) results in better spatial resolution and fewer beam-filling problems than the Defense Meteorological Satellite Program (DMSP). The TMI is a nine-channel passive radiometer with dual (vertical, V, and horizontal, H) polarization channels at 10.7, 19.4, 37 and 85.5 GHz and a vertical polarization channel at 21.3 GHz. A description of the field of view (FOV) for TMI channels was introduced by Kummerow *et al.* (1998). The TMI data used in this study are the TMI version-5 Level-1B11 low resolution Tbs. The spatial resolution is about 10 km (Hong *et al.*, 1999). The Level-1B11 data were the instrument data in full resolution with calibration and Earth location computed (Simpson *et al.,* 1996). The TRMM Science Data and Information System (TSDIS) and the TRMM office processed the data. These data are archived and distributed by the Goddard Distributed Archive Center (GDAC). Considering the spatial resolution of the level-1B11 data, the match-up definition of a gauge measurement and its corresponding TMI Tbs is that the distance measured from the center of the effective field of view to ground-based station is within 5 km and its temporal difference is within 1 hour.

The Central Weather Bureau (CWB) of Taiwan also provided hourly rain measurements from three islands: Pengchiayu (25.62^{o}N, 122.07^{o}E), Lutao (22.65^{o}N, 121.47^{o}E), and Lanyu (22.04^{o}N, 121.55^{o}E). The JMA provided oceanic rainfall data from nine islands in the

study domain ncluding (table 1): MIYAKOJIMA (station #93041), TARAMA (#93061), IBARUMA (#94001), YONAGUNIJIMA (#94017), KABIRA (#94036), IRIOMOTELIMA (#94061), ISHIGAKIJIMA (#94081), OHARA (#94101), and HATERUMA (#94116). The data time step was 10 minutes. Rain gauge data from these islands were treated as ground truth data, and were used to establish linear regression equations between the island RRs and coinciding MW Tbs.

2.2 *Algorithm*

The radiative transfer processes of rain can be separated into two regimes: the attenuation and scattering regimes. The microwave Tbs observed in the attenuation regimes represent observations of the liquid hydrometeors within the raining cloud, which can be considered direct rainfall measurements. On the other hand, the microwave Tbs observed in the scattering regime depends on the many details of the ice layer. The satellite microwave Tbs thus can be divided into attenuation-based and scattering-based measurements. The factors determining the type of attenuation encountered include precipitation particle size, particle phase (ice or liquid), and the radiation wavelength (Chen and Li, 2002a).

This study considered the limb-corrected problem of the AMSU-A data by discarding the furthest three pixels on each scanning side. Since the value of the scanning view angle might not be the same for all AMSU-A raining pixels, and since little water vapor exists in the path from the cloud-top to the satellites, a slight difference is caused by the attenuation of water vapor above the top of the raining cloud to the radiometer of the satellite. The rain threshold for the AMSU-A channel was determined using the AMSU-A Tb statistic of demonstrating no rain events from island stations. In this study, the rain thresholds are taken as the mean values of the Tb. These thresholds were 208.37, 179.42, and 254.56 K for the Tb23, Tb31, and Tb89 respectively. Island rain gauge data can be used as ground-truth data coincident with the satellite rainfall observations (Chen and Li, 2000). In this study, rain gauge observations were treated as the rain representatives for the waters around the associated island. Because the island area is smaller than AMSU-A FOV, this study does not consider the island land effect on rainfall retrieval.

In this study rainfall observations were treated as the rainfall representatives for the waters around the associated island. Because, in length, the dynamic ranges of TMI channels are different, in general, it is longer for a TMI channel at lower frequency (Hong *et al*., 1999). Within the dynamic range, the relationship between RR and TMI Tb is near linear. Within this rainfall algorithm, the entire rainfall range is composed of many piecewise linear regression intervals, and the number of TMI channels within each interval is different. The key point of this rainfall algorithm is to determine which TMI channel can join the multiple-linear regression within a specific piecewise linear regression interval(Chen and Li, 2002b). The relationship between RR and TMI multiple Tbs in this interval is highly linear. This yields a one-to-one function. The island land effect on the rain retrieval must be evaluated where an island exists within the TMI FOV. The land effects of eight islands within the study domain on the passive microwave measurements were examined in this paper. The first island is Tarama Jima in the Sakishima Gunto (Japan). In addition, there are seven island stations around Taiwan. From north to south, they are Pengchiayu, Penghu, Tungchitao, Lutao, Liuchiu, Lanyu and Dongsh Island. According to comparison results (not shown in this paper) of the island no-rainfall statistics and buoy no-rainfall statistics, Tarama Jima, Tungchitao, Pengchiayu, and Dongsha Island were chosen for rainfall characteristic monitoring due to their minor island land effect. The hourly rain measurements from Pengchiayu and Dongsha Island were used to establish the linear regression equations with their coincident TMI data. The hourly rain measurements from Tarama Jima and Tungchitao were used as ground-truth data for quantitatively verifying the rain retrievals using the TMI.

Accurate rain identification determines the efficiency of rain retrievals using satellite-based passive microwave radiometers. A rain identification technique's duty is to accurately distinguish the rain signal from environmental noise. The scattering Index (SI) technique using the TMI for identifying oceanic rainfalls was used in this paper. The SI technique originally developed for the SSM/I rain rate estimation technique for recognizing rainy scenes over the oceans (Goodberlet *et al.,* 1989, 1990). By using the multi-channel microwave data from the SSM/I, Grody (1991) used the decision tree method to classify snow cover and precipitation. His study result was improved upon by Ferraro *et al*. (1994) for presenting the effects of surface conditions on rain identification. For global applications, a value of SI greater than 10 K indicates the presence of both scattering and emission due to rain and generally corresponds to rain rates of 1 mm/h or greater. The SI technique proved adequate performance in the detection of rain areas. A rainy TMI measurement whose Tb85V and Tb85H are lower than their no-rainfall thresholds was classified as a rain scene associated with scattering-based mechanism due to the scattering characteristics of these channels.

Otherwise, it is a rainy event associated with the attenuation-based mechanism.

3. SUMMAY

The existing individual microwave radiometer currently cannot provide enough measurements to monitor typhoons occurring at sea, so the best policy is using multi-microwave channels, which were on board different platforms to obtain rainfall rate. Inter-calibration between the rainfall rates should be performed before we combining the rain retrievals from various satellite radiometers.

This study developed an oceanic rainfall algorithm for typhoons occurred near Taiwan using the AMSU-A channels at 23.8, 31.4, and 89.0 GHz. Validation of rain identification was carried out using rain gauge data. As for quantitative validation, the coefficient of determination is better than 0.7. The algorithm developed in this study was to be suitable for retrieving the rainfall rate at sea (see Fig.1 and Fig.2). Also, the TMI RR retrieval result showed a moderate performance in comparison with the AMSU-A RR retrievals. Since the study results showed good agreement in qualitative comparisons between TMI RR and AMSU-A RR, and since the intensities of AMSU-A RRs roughly equaled to the TMI RRs when multiplied by a factor, especially true for heavy rainfalls, good potential exists for establishing a dual-satellite rainfall observation system using both AMSU-A and TMI instruments. In the future the Precipitation Radar instrument is expected to be included in the observation system.

Additionally, using the real-time data from the AMSU-A should obtain better quantitative estimates of heavy rainfall and enable new knowledge to be obtained in the study of typhoons. The study results also showed that the optimal advantage of this statistical approach is the simplicity of the calculations involved. Further improvement of this algorithm would be helpful for accurately estimating rainfall rates over ocean areas.

4. REFERENCE

Chen, W. J. and C. C. Li, 2000: Oceanic Rain Rate Retrievals Using TRMM Microwave Imager Multi-Channel Brightness Temperatures During the 1998 SCSMEX, *TAO,* **11**, 765-788.

Chen, W. J. and C. C. Li, 2002a: An infrared rainfall algorithm for the MCSs prevailing over the South China Sea during the Mei-Yu season, *TAO*, **13**, 65-90.

Chen, W. J. and C. C. Li, 2002b: Rainfall retrievals using Tropical Rainfall Measuring Mission and Geostationary Meteorological Satellite 5 data obtained during the SCSMEX, *Inter. J. of Remo. Sens.*, **23**, 2425-2448.

Ferraro, R. R., N. Grody, and G. F. Marks, 1994: Effects of surface conditions on rain identification using the DMSP-SSM/I. *Remote Sens. Rev.*, **11**, 195-209.

Goodberlet, M. A., C. T. Swift, and J. C. Wilkerson, 1989: Remote sensing of ocean surface winds with the Special Sensor Microwave/ Imager. *J. Geophys. Res.*, **94**, C10, 14547-14555.

Goodberlet, M. A., C. T. Swift, and J. C. Wilkerson, 1990: Ocean surface wind speed measurements of the Special Sensor Microwave/ Imager (SSM/I). *IEEE Trans. Geosci. Remote Sens*., **28**, 823-827.

Grody, N. C., F. Weng and R.R. Ferraro, 1999: Application of AMSU for Obtaining Hydrological Parameters, Microwave Radiometry and Remote Sensing of the Earth's Surface and Atmosphere, *VNU Science Press*, Brill Academic Publishers, Inc., pp.339-351.

Grody, N. C., 1991: Classification of snow cover and precipitation using the Special Sensor Microwave Imager. *J. Geophys. Res.,* **96,** 7423-7435.

Hong, Y., C. D. Kummerow, and W. S. Olson, 1999: Separation of convective and stratiform precipitation using microwave brightness temperature. *J. Appl. Meteor.,* **38**, 1195-1213.

Kummerow C., 1998: Beam-filling errors in passive microwave rainfall retrievals, *J. Appl. Meteor*., **37**, pp.356-370.

Kummerow, C., W. Barnes, T. Kozu, J. Shiue, and J. Simpson, 1998: The tropical rainfall measuring mission (TRMM) sensor package. *J. Atmos. Oceanic. Technol*, **15**, 809-817.

Richards, J. A. and X. Jia, 1999: *Remote Sensing Digital Image Analysis- An Introduction*, Springer, 363pp.

Simpson, J., C. Kummerow, W. K. Tao, and R. F. Adler, 1996: On the tropical rainfall measuring mission （TRMM）. *Meteor. Atmos. Phys.*, **60**, 19-36.

Wilheit, T. T. and A. T. C. Chang, 1980: An algorithm for retrieval of ocean surface and atmospheric parameters from the observations of the scanning multi-channel microwave radiometer. *Radio Sci.*, **15**, 525-544.

Table. 1 Locations of JMA island stations.

Rain Gauge Station	Code of Station	North Lat. East Lon.	Altitude（m）
MIYAKOJIMA	93041	24.79N 125.28E	40
TARAMA	93061	24.67N 124.70E	16
IBARUMA	94001	24.50N 124.28E	15
YONAGUNIJIMA	94017	24.46N 123.01E	30
KABIRA	94036	24.46N 124.14E	7
ISHIGAKIJIMA	94081	24.33N 124.16E	6
IRIOMOTEJIMA	94061	24.39N 123.75E	9
OOHARA	94101	24.26N 123.87E	28
HATERUMA	94116	24.05N 123.76E	32
PENGCHIAYU	46695	25.62N 122.07E	101

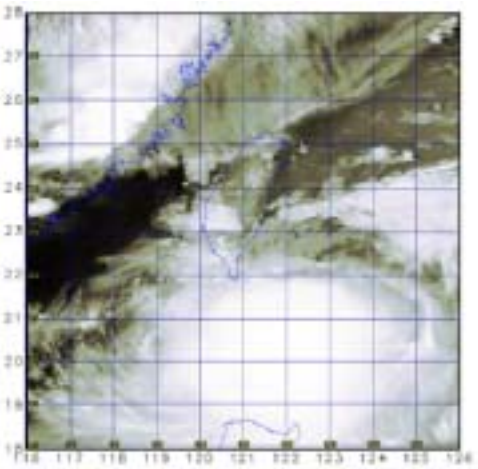

Fig. 1 AVHRR IR4 image of Typhoon TRAMI at 1120UTC on 11 July, 2004.

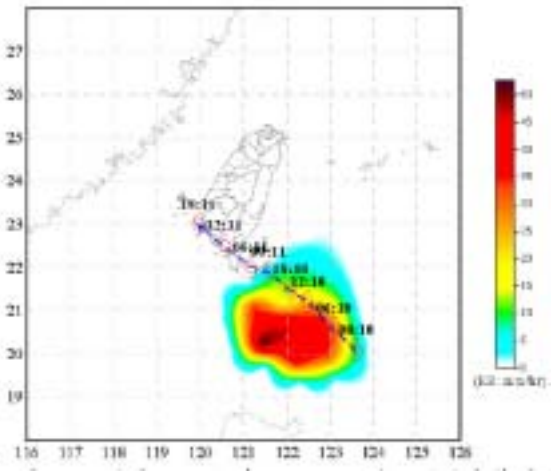

Fig. 2 AMSU-A RR retrievals of Typhoon TRAMI at 1120UTC on 11 July, 2004.